CHAPTER 2

HOLLOW CORE WAVEGUIDES

2.1 BASIC CHARACTERISTICS

Hollow-core waveguides (HCWs) are comprised of a central hole surrounded by a highly reflective inner wall.

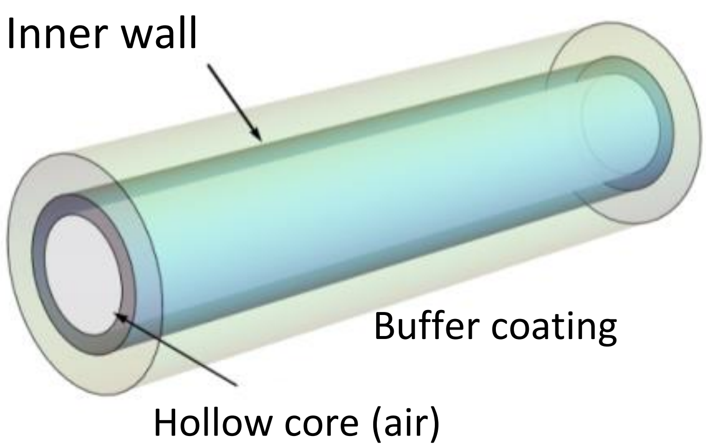

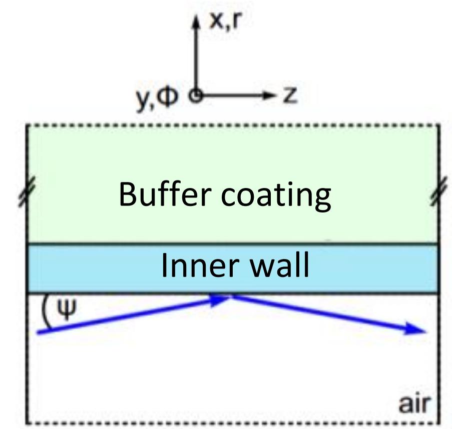

The core can be filled with air, inert gas, liquid, or vacuum, allowing these waveguides to transmit a broad range of wavelengths with low attenuation.

HCWs are of particular interest for the transmission of infrared (IR) to THz radiation, where it is otherwise difficult to find materials that have the optical, thermal, and mechanical properties required for use in solid-core optical fibers.

Therefore, IR-transmitting hollow waveguides can be an attractive alternative to solid-core IR fibers.

2.1 BASIC CHARACTERISTICS

The concept of using hollow pipes to guide electromagnetic waves was first described by Rayleigh in 1897

XVIII. *On the Passage of Electric Waves through Tubes, or the Vibrations of Dielectric Cylinders.* By LORD RAYLEIGH, *F.R.S.**

General Analytical Investigation.

THE problem here proposed bears affinity to that of the vibrations of a cylindrical solid treated by Pochhammer† and others, but when the bounding conductor is

* Communicated by the Author.
† Crelle, vol. xxxi. 1876.

Phil. Mag. S. 5. Vol. 43. No. 261. *Feb.* 1897. L

Further understanding of hollow waveguides was delayed until the 1930s when microwave-generating equipment was first developed and hollow waveguides for these wavelengths were constructed.

The success of these waveguides inspired researchers to develop hollow waveguides to the IR region.

Initially these waveguides were developed for medical uses especially high-power laser delivery.

Later on, they have been used to transmit incoherent light for broadband spectroscopic and radiometric applications.

2.1 BASIC CHARACTERISTICS

Hollow waveguides present several **advantages** over solid-core optical fibers

- ✓ ability to transmit wavelengths well beyond 20 µm
- ✓ high-power laser delivery
- ✓ high laser power damage thresholds
- ✓ simple structure
- ✓ low nonlinear effects
- ✓ low insertion loss (no Fresnel reflections from the end face of an HCW when radiation is coupled from free space into the air core);
- ✓ no end reflection
- ✓ small beam divergence
- ✓ potentially low cost

Potential **disadvantages** include:

- ❑ additional loss on bending
- ❑ small numerical aperture (NA)

2.2 ATTENUATED TOTAL INTERNAL REFLECTION

HCWs can be classified into two categories: **attenuated total internal reflection** (ATIR) waveguides and **leaky-type** HCWs.

ATIR waveguides guide light by total internal reflection in the same manner as core/cladding optical fiber.

Since for solid fiber $n_{core} > n_{clad}$, ATIR waveguides should consist of a hollow core surrounded by wall material with a refractive index $n_{clad} < 1$ for the transmitted wavelength.

How is it possible to have solid materials with a refractive index lower than one, to be used as cladding for an ATIR waveguide?

The absorption profile $\alpha(\omega)$ of a material can be obtained from the classical model of a damped oscillator with charge q under the influence of a driving force $q\vec{E}$ caused by the incident wave with amplitude $\vec{E} = E_0 e^{i\omega t}$

By combining the Lamber-Beer law $I = I_0 e^{-\alpha(\omega)z}$ with the Maxwell equation $\vec{P} = \varepsilon_0(\varepsilon - 1)\vec{E}$, where $\vec{P}$ is the polarization vector and ε_0 is the dielectric constant, the real n' and imaginary part κ of the refractive index $n = n' - i\kappa$ can be determined as a function of the angular frequency ω

2.2 ATTENUATED TOTAL INTERNAL REFLECTION

leading to the Kramers–Kronig dispersion relations for the absorption coefficient $\alpha = 2k_0\kappa$ proportional to the imaginary part of the refractive index (known as extinction coefficient)

$$\alpha = \frac{Ne^2}{4\varepsilon_0 mc}\frac{\left(\frac{\gamma}{2}\right)}{(\omega_0-\omega)^2+\left(\frac{\gamma}{2}\right)^2}$$

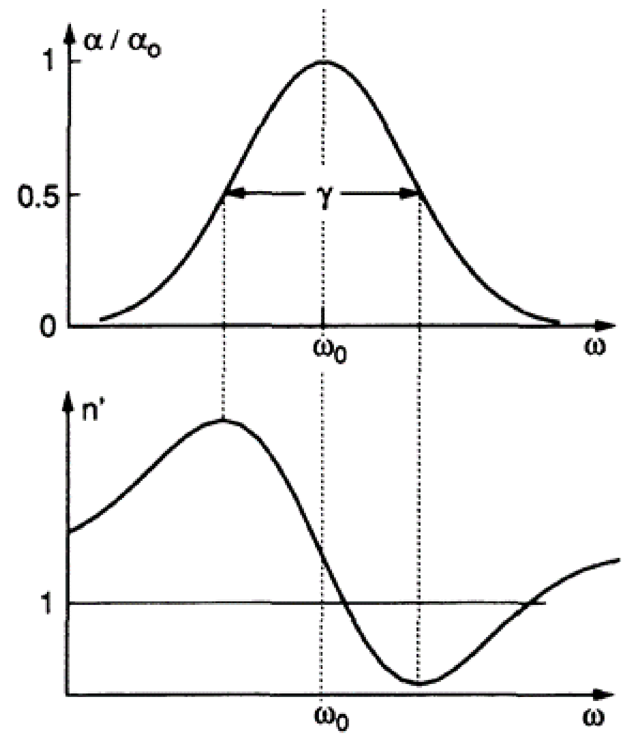

and for the real part of the refractive index

$$n' = 1 + \frac{Ne^2}{4\varepsilon_0 m\omega_0}\frac{\omega_0-\omega}{(\omega_0-\omega)^2+\left(\frac{\gamma}{2}\right)^2}$$

where N is the total number of molecules, m is the mass of the electron, c is the speed of light, γ is the natural linewidth and ω_0 is the angular frequency of a radiative transition.

2.2 ATTENUATED TOTAL INTERNAL REFLECTION

The absorption profile $\alpha(\omega)$ is Lorentzian with a Full-Width-Half-Maximum (FWHM) of γ, which equals the natural linewidth of the optical transition.

We observe that the real part n' of refractive index is always positive ω_0, except close to a resonant frequency.

The spectral region in which a material has $n' < 1$ is called the **anomalous dispersion region**.

In this region the absorption coefficient α is high and therefore the evanescent waves that propagate in the wall material are absorbed due to the high absorption within the inner wall, limiting the performance of the ATIR guides.

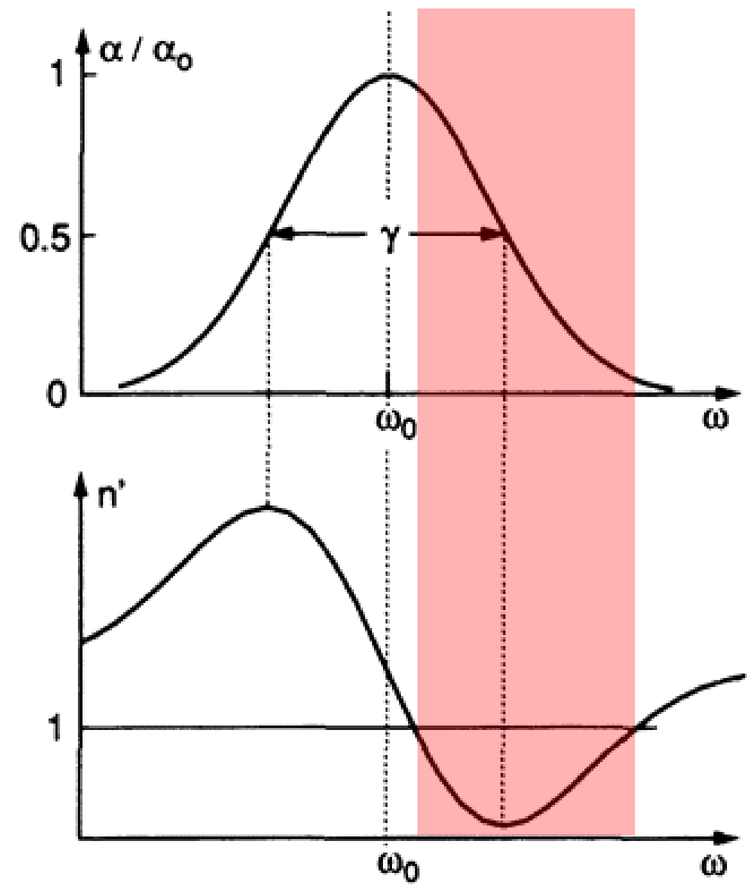

2.3 METALLIC/DIELETRIC COATING

The other type of HCW utilizes a highly reflective wall to confine light to the hollow core.

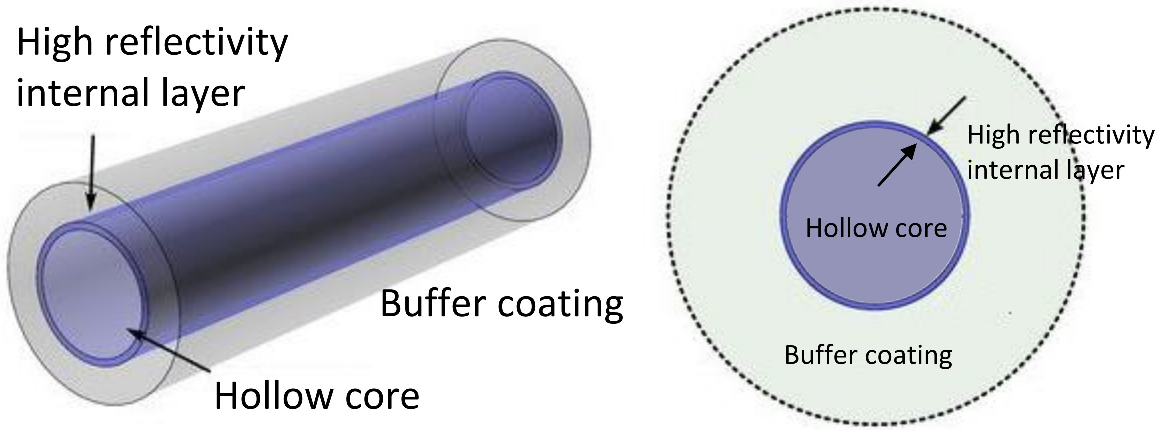

Leaky modes propagate in these HCWs since the wall is not a perfect reflector; thus, they are referred to as leaky-type HCWs.

Increasing the wall's reflectivity increases the degree to which light is confined to the waveguide's hollow core, thus decreasing the attenuation of radiation propagating along its axis.

Leaky-type HCWs can be divided into different categories based upon how the wall of the waveguide is designed to achieve high reflectivity.

2.3 METALLIC/DIELETRIC COATING

The most basic design is to use a smooth metal surface to form the inner wall of the waveguide.

This can be accomplished using a metal tube or by depositing a metal film on the smooth inner surface of a glass or plastic tube.

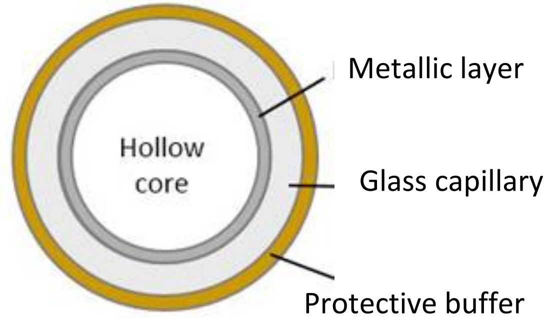

However, the reflectivity of metallic surface also strongly depends on the conditions of the irradiated surface.

A dielectric layer is then added over the metal to provide enhanced reflectivity within specific wavelength ranges due to an interference effect.

These waveguides are called **metal/dielectric HCWs**.

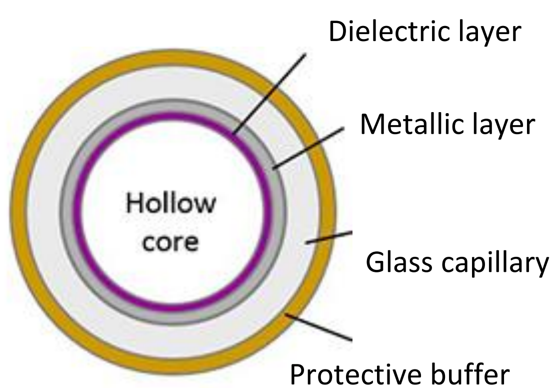

2.3 METALLIC/DIELETRIC COATING

The basic principle is based on Bragg diffraction.

Let us a suppose a vertical incidence of the electric field with amplitude E_0, that means that the we are considering a pure transverse mode in the HCW (longitudinal component of the electric field is negligible).

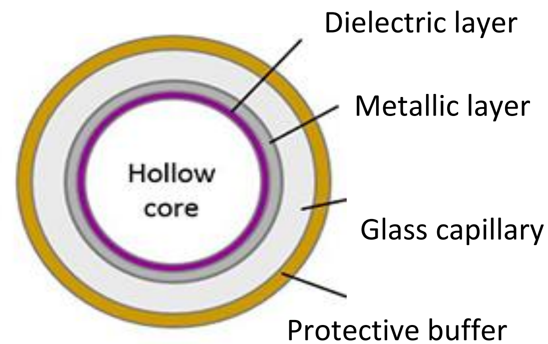

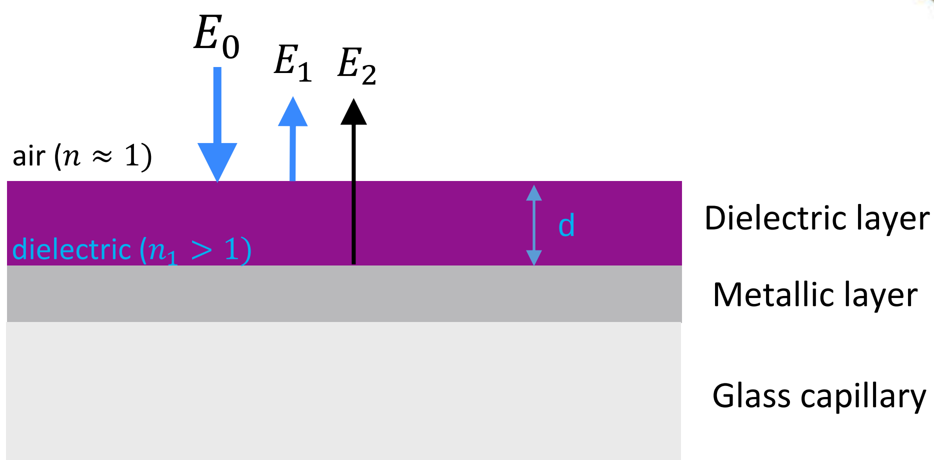

E_1 is the amplitude of the reflected mode at the interface air/dielectric

E_2 is the amplitude of the reflected mode at the interface dielectric/metal after emerging from the dielectric layer.

For constructive interference, the phase difference between E_1 and E_2 has to be:

$$\delta_m = 2m\pi \qquad \text{with } m = 1,2,3,\ldots$$

2.3 METALLIC/DIELETRIC COATING

Let us assume that the metal has a high reflectivity ($R > 0.9$).

The focus in on the interface air/dielectric.

The reflectivity of a plane interface between two regions with complex refractive indices $n = n' - i\kappa$ (air) and $n_1 = n'_1 - i\kappa_1$ (dielectric can be calculated from Fresnel's formulas.

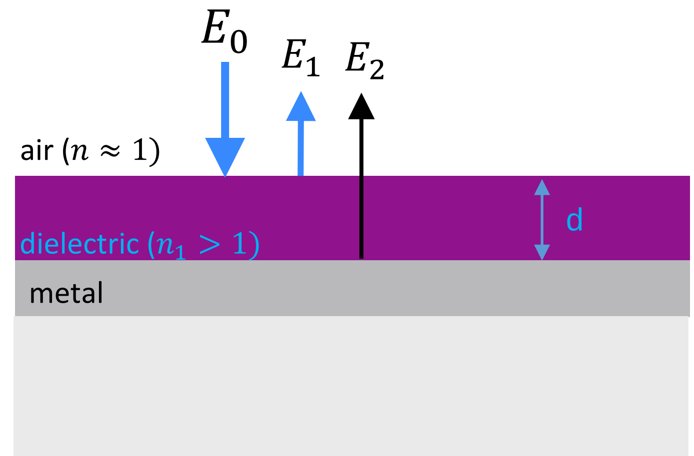

It depends on the angle of incidence and on the direction of polarization.

For vertical incidence, one obtains from Fresnel's formulas:

$$R = \left(\frac{n - n_1}{n + n_1}\right)^2$$

To achieve maximum reflectivities, the numerator $(n - n_1)^2$ should be maximized and the denominator minimized. Since $n \approx 1$, this implies that n_1 should be as large as possible.

2.3 METALLIC/DIELETRIC COATING

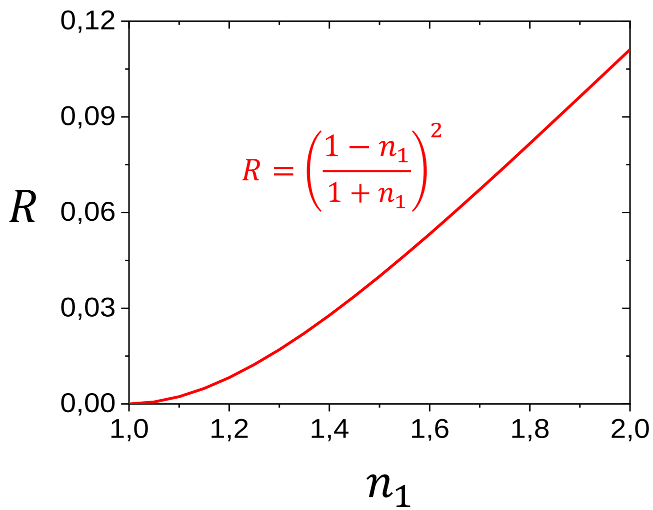

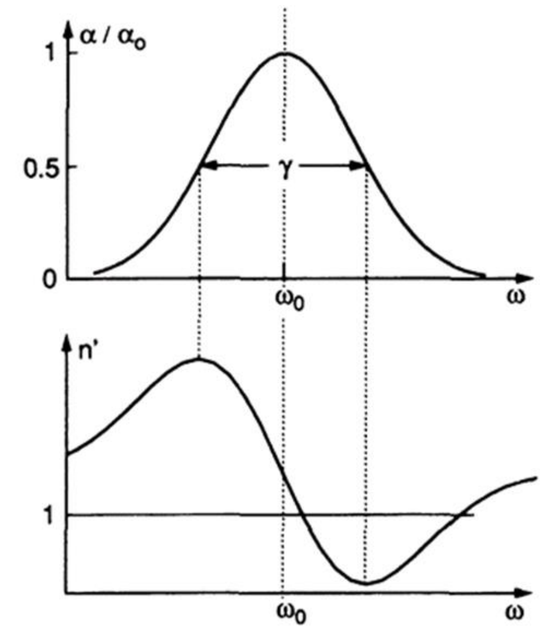

Unfortunately, the Kramers-Kronig dispersion relations imply that a large value of n also causes large absorption.

The situation can be improved by selecting reflecting materials with low absorption (which then necessarily also have low reflectivity) but using many layers with alternating high and low refractive index.

Choosing the proper optical thickness $n_i d$ of each layer allows constructive interference between the different reflected amplitudes to be achieved.

Reflectivities of up to R > 99.9 % can been reached.

2.3 METALLIC/DIELETRIC COATING

Multilayer metal/dielectric HCWs are fabricated by adding multiple dielectric layers over the metal to form an alternating high/low refractive index structure.

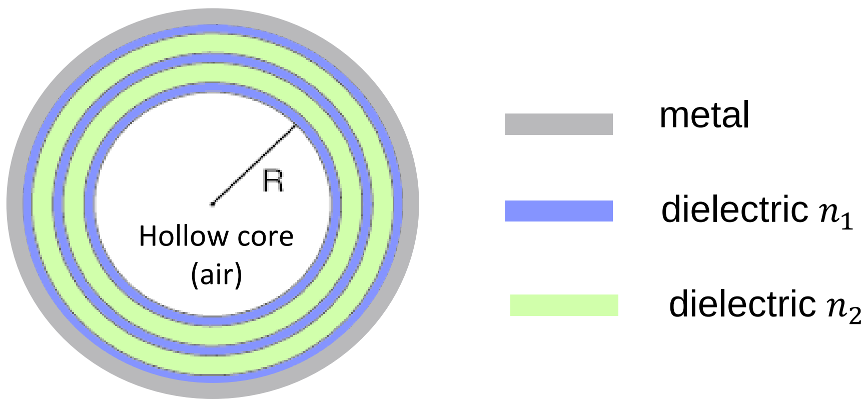

Let us consider the simplest case composed by two dielectrics, with $n_1 > n_2$.

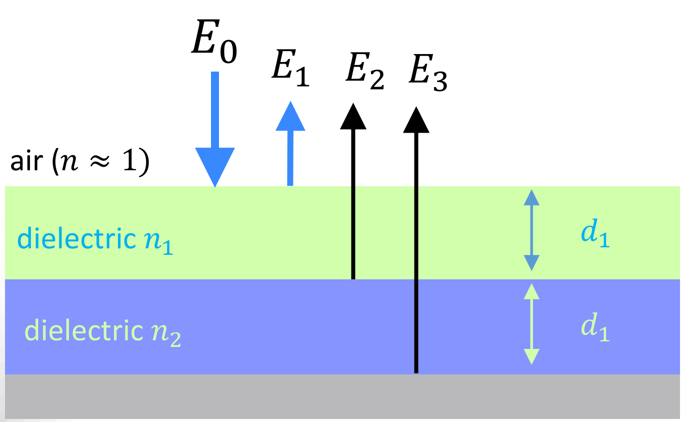

E_1 is the amplitude of the reflected mode at the interface air/dielectric n_1

E_2 is the amplitude at the interface dielectric n_1 /dielectric n_2, after emerging in air

E_3 is the amplitude at the interface dielectric n_2/metal, after emerging in air

2.3 METALLIC/DIELETRIC COATING

The phase differences between all reflected components have to be:

$$\delta_m = 2m\pi \qquad \text{with } m = 1,2,3,\ldots$$

for constructive interference.

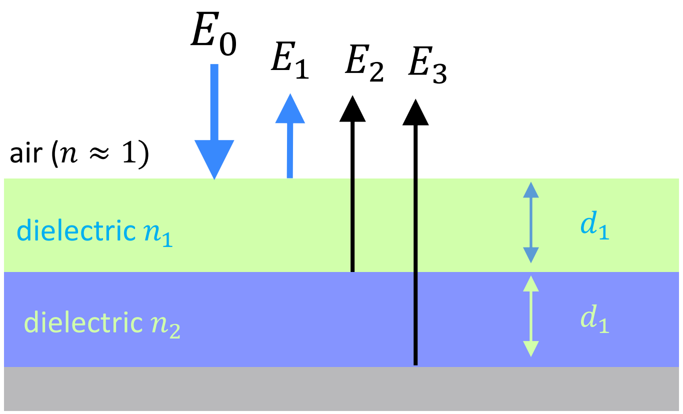

Taking into account the phase shift $\delta = \pi$ at reflection from an interface with a larger refractive, we obtain the condition for the total phase shift between $\overrightarrow{E_1}$ and $\overrightarrow{E_2}$:

$$\delta_{(m=1)} = \frac{2\pi}{\lambda}\Delta s + \pi = \frac{2\pi}{\lambda}2n_1 d_1 + \pi = 2\pi$$

that implies: $n_1 d_1 = \dfrac{\lambda}{4}$

Similarly, the total phase shift between $\overrightarrow{E_2}$ and $\overrightarrow{E_3}$ is:

$$\delta_{(m=1)} = \frac{2\pi}{\lambda}\Delta s + \pi = \frac{2\pi}{\lambda}(2n_2 d_2) + \pi = 2\pi$$

that again implies: $n_2 d_2 = \dfrac{\lambda}{4}$

2.3 METALLIC/DIELETRIC COATING

$$n_1 d_1 = \frac{\lambda}{4}$$ $$n_2 d_2 = \frac{\lambda}{4}$$

The thickness on the dielectric coatings can be optimized for a specific wavelength.

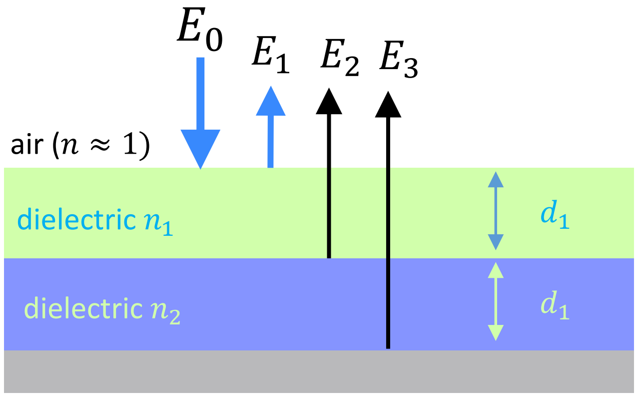

The reflected amplitudes can be calculated from Fresnel's formulas.

The total reflected intensity is obtained by summation over all reflected amplitudes taking into account the correct phase.

The refractive indices are now selected such that $\sum_i E_i$ becomes a maximum.

The calculation is still feasible for our example of a two-layer coating and yields for the three reflected amplitudes (double reflections are neglected)

$$E_1 = \sqrt{R_1} E_0$$
$$E_2 = \sqrt{R_2}\left(1 - \sqrt{R_1}\right) E_0$$
$$E_3 = \sqrt{R_\mathrm{m}}\left(1 - \sqrt{R_2}\right)\left(1 - \sqrt{R_1}\right) E_0$$

$$R_1 = \left(\frac{1 - n_1}{1 + n_1}\right)^2$$
$$R_2 = \left(\frac{n_2 - n_1}{n_2 + n_1}\right)^2$$

where the reflectivities R_i are given by Fresnel's formula and R_m is the reflectivity of the metal layer.

2.3 METALLIC/DIELETRIC COATING

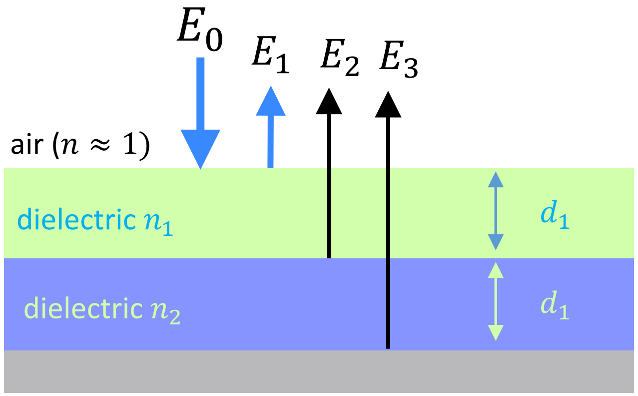

Let us assume for example:

$$|n_1| = 1.6$$

$$|n_2| = 1.2$$

$$R_\mathrm{m} = 0.9$$

Then, reflectivitiy can be estimated by using Fresnel's formula:

$$R_1 = \left(\frac{1 - n_1}{1 + n_1}\right)^2 = 0.05$$

$$R_2 = \left(\frac{n_2 - n_1}{n_2 + n_1}\right)^2 = 0.02$$

The amplitude for the partial electric fields results:

$$E_1 = \sqrt{R_1}E_0 = 0.23E_0$$

$$E_2 = \sqrt{R_2}\left(1 - \sqrt{R_1}\right)E_0 = 0.11E_0$$

$$E_3 = \sqrt{R_\mathrm{m}}\left(1 - \sqrt{R_2}\right)\left(1 - \sqrt{R_1}\right)E_0) = 0.63E_0$$

2.3 METALLIC/DIELETRIC COATING

The total amplitude will be:

$$E_R = \sum_i E_i = 0.97 E_0$$

This corresponds to a total reflectivity of the multi-layer structure, which is higher than the reflectivity of the metallic layer $R_{\mathrm{m}} = 0.9$:

The total intensity reflected by the multi-layer structure will be:

$$I_R = 0.97^2 I_0 = 0.93 I_0$$

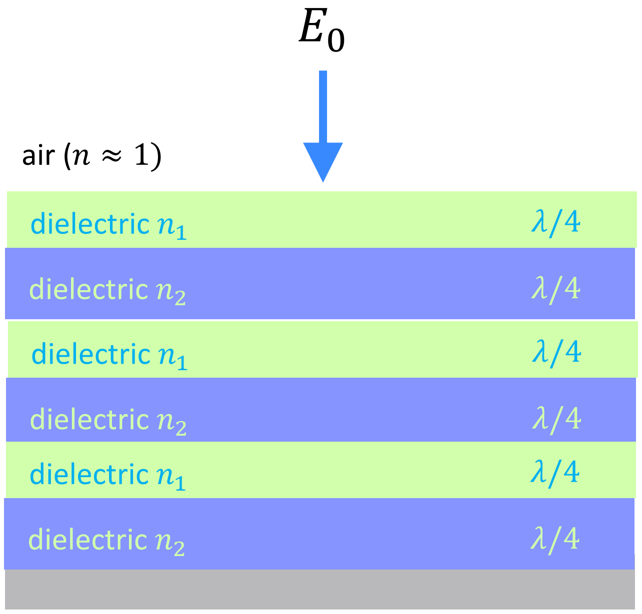

This example suggests that for materials with low absorption, more layers can be used to achieve a reflectivity even higher.

The calculation and optimization of multilayer coatings with up to 20 layers becomes very tedious and time consuming, and is therefore performed using computer programs

2.3 METALLIC/DIELETRIC COATING

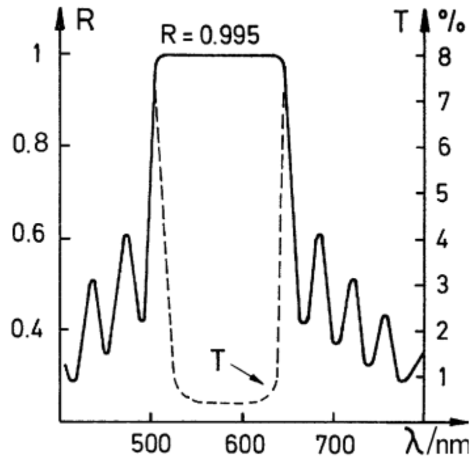

Reflectivity of a high-reflectance multilayer mirror with 17 layers as a function of the incident wavelength λ

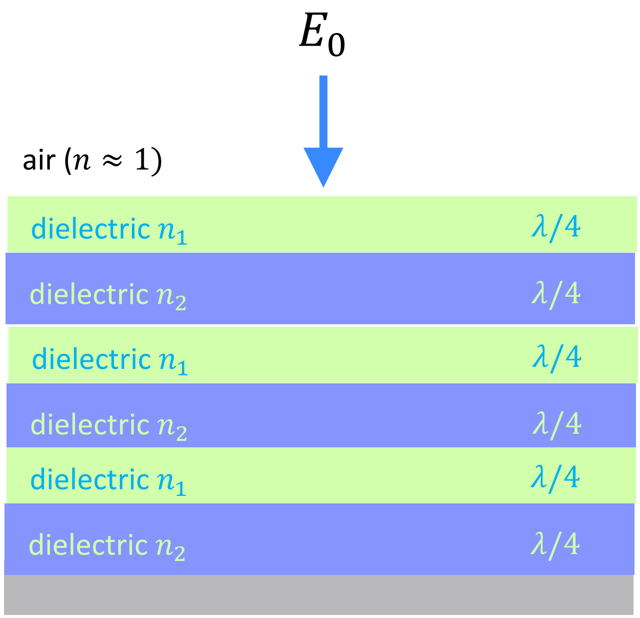

By proper selection of different layers with slightly different optical path lengths, one can achieve a high reflectivity over an extended spectral range.

At such low absorption losses, the scattering of light from imperfect mirror surfaces may become the major loss contribution.

Such dielectric mirrors with alternating $\lambda/4$-layers of materials with high and low refractive indices are often called “Bragg reflectors” because they work in a similar way to the Bragg reflection.

2.3 METALLIC/DIELETRIC COATING

2.3.1 Selection of metal

The complex refractive index of metal is defined as

$$N = n - i\kappa$$

where n is the refractive index and k is the extinction coefficient.

The figure of merit:

$$F = \frac{n}{n^2 + \kappa^2}$$

is the quantity used to characterize the performance of the waveguide, which is a measure of metal's reflectivity.

For metals, the figure of merit is inversely proportional to its reflectivity.

Commonly used metals for high reflection coatings are silver, gold, aluminum, and copper.

In order to estimate the figure of merit F we need to know the real and imaginary part or the refractive index of these metals.

2.3 METALLIC/DIELETRIC COATING

2.3.1 Selection of metal

Optical properties of the metals Al, Co, Cu, Au, Fe, Pb, Ni, Pd, Pt, Ag, Ti, and W in the infrared and far infrared

M. A. Ordal, L. L. Long, R. J. Bell, S. E. Bell, R. R. Bell, R. W. Alexander, Jr., and C. A. Ward

Infrared optical constants collected from the literature are tabulated. The data for the noble metals and Al, Pb, and W can be reasonably fit using the Drude model. It is shown that $-\epsilon_1(\omega) = \epsilon_2(\omega) \simeq \omega_p^2/(2\omega_\tau^2)$ at the damping frequency $\omega = \omega_\tau$. Also $-\epsilon_1(\omega_\tau) \simeq -(\frac{1}{2})\,\epsilon_1(0)$, where the plasma frequency is ω_p.

1 April 1983 / Vol. 22, No. 7 / APPLIED OPTICS

By using n and κ values listed in this paper, the figure of merit $1/F$ has been and plotted as a function of wavelength in the infrared range.

Minimum loss in the infrared range can be achieved by choosing either **silver** (Ag) with $F \approx 10^{-3}$ or gold (Au) with $F \approx 0.7 \cdot 10^{-2}$, due to their lower figure of merit values.

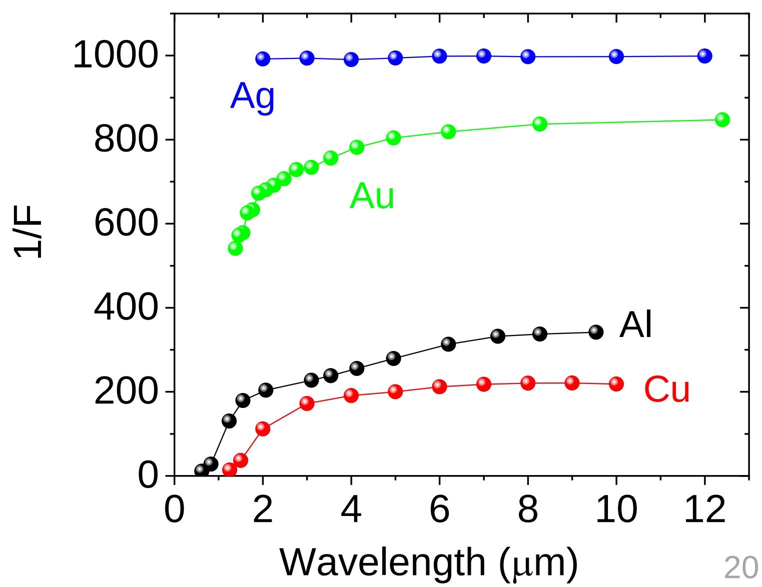

2.3 METALLIC/DIELETRIC COATING

2.3.2 Selection of dielectric

Hollow core metal coated waveguides utilize a highly reflective wall to confine light to the air core.

By increasing the wall's reflectivity, the degree to which light is confined to the waveguide's air core increases, thus decreasing the attenuation of radiation propagating along its axis.

Since the wall is not a perfect reflector, leaky modes tend to propagate in these hollow silver or gold coated waveguides.

A dielectric layer is then added over the metal to improve reflectivity within specific wavelength ranges due to the interference effect.

For the dielectric, the attenuation coefficient varies directly as the figure of merit F_d, which is a function of the dielectric material's complex refractive index $N_d = n_d - i\kappa_d$:

$$F_d = \frac{1}{2}\left(\frac{N_d^2}{\sqrt{N_d^2 - 1}}\right)^2$$

2.3 METALLIC/DIELETRIC COATING

2.3.2 Selection of dielectric

$$F_d = \frac{1}{2}\left(\frac{N_d^2}{\sqrt{N_d^2 - 1}}\right)^2$$

$$N_d = n_d - i\kappa_d$$

The optimum value of n_d can be calculated by assuming a lossless dielectric (extinction coefficient $\kappa_d = 0$).

In the picture, F_d is plotted as a function of n_d, assuming $\kappa_d = 0$.

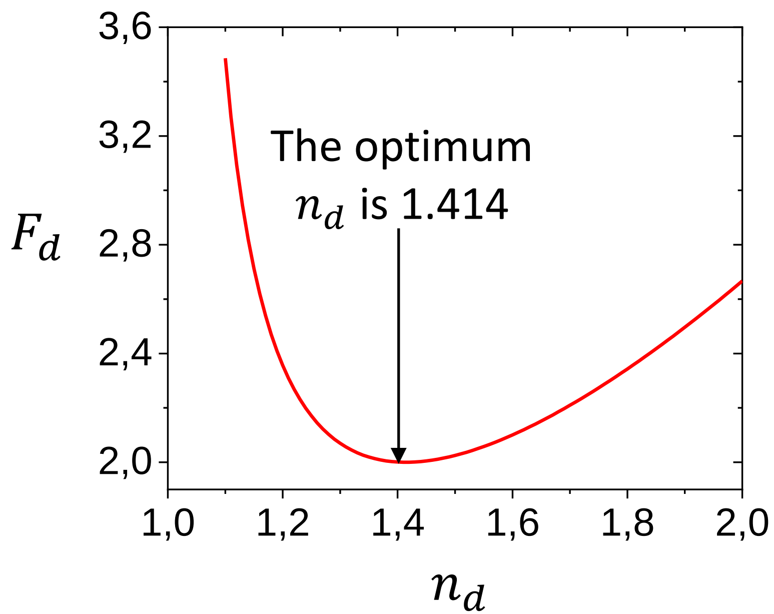

2.3 METALLIC/DIELETRIC COATING

2.3.2 Selection of dielectric

Several kinds of material have been used in the hollow fibers as the dielectric inner coating layer to enhance the reflection rate and thus lower the loss.

Among these dielectric materials, **silver iodide** (AgI) is one of the best coatings for infrared regions, showing a $\kappa_d < 10^{-3}$.

Specifically, for an AgI layer with $\kappa_d{\sim}10^{-3}$, the transmission loss increases by 2.4%/m over a lossless dielectric.

Hence the AgI film has almost ideal properties in the mid IR, as the losses for the AgI films of thickness less than 1 m are extremely small.

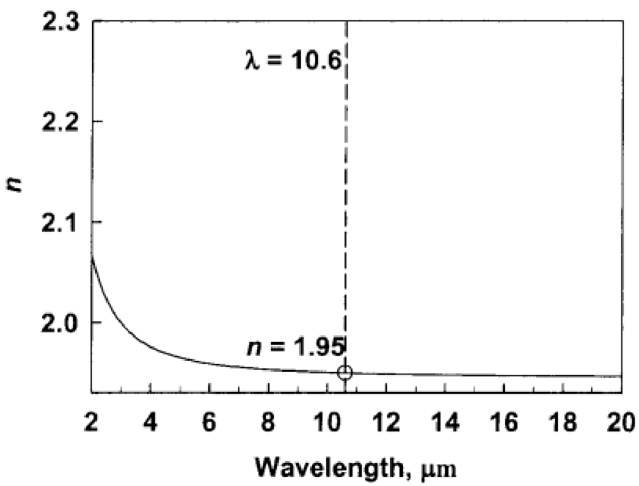

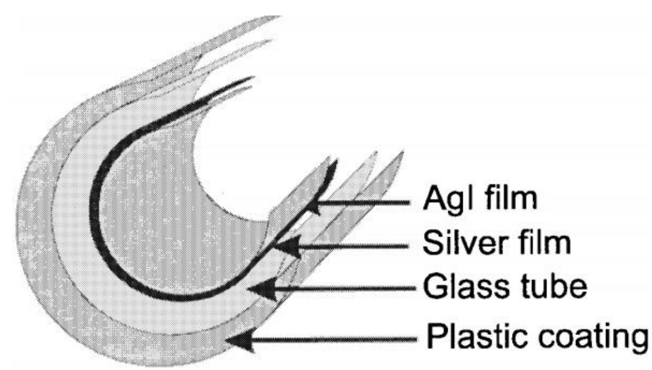

2.3 METALLIC/DIELETRIC COATING

2.3.2 Selection of dielectric

…and what about longer wavelengths?

Is there any chance to use hollow core waveguides in THz range ($\lambda > 50\mu m$)?

Which metal/dielectric coating can be used?

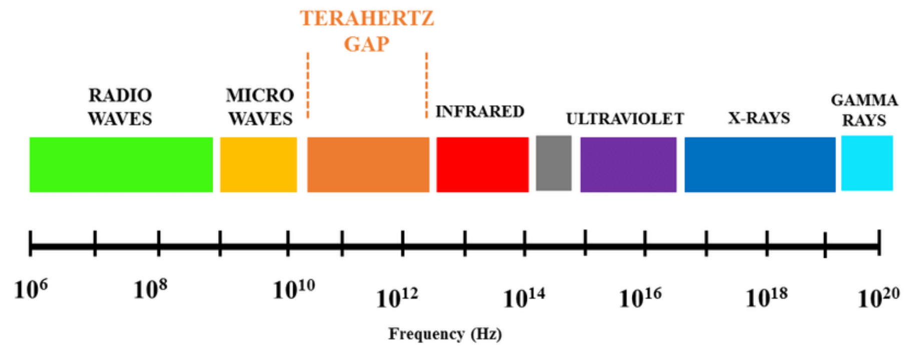

For metal, let's use the same figure of merit $1/F$ to measure of metal's reflectivity

$$F = \frac{n}{n^2 + \kappa^2}$$

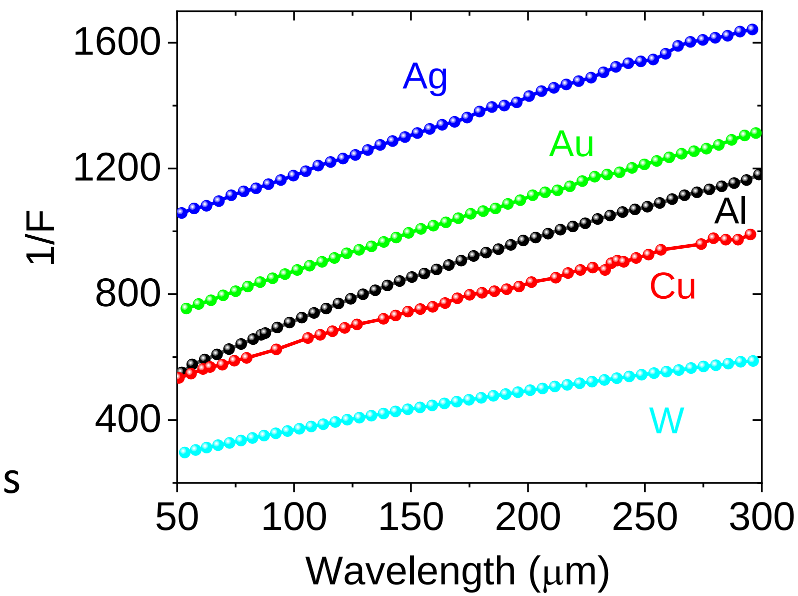

Silver is the best solution, as for the infrared range.

2.3 METALLIC/DIELETRIC COATING

2.3.2 Selection of dielectric

Polystyrene (PS) was chosen to be the dielectric, due to its low extinction coefficient, which enhances the transmission through the waveguide.

Also, polystyrene has a complex refractive index of $1.58 - i3.58 \cdot 10^{-3}$, within the dielectric's optimal range.

October 15, 2007 / Vol. 32, No. 20 / OPTICS LETTERS

Silver/polystyrene-coated hollow glass waveguides for the transmission of terahertz radiation

Bradley Bowden,[1] James A. Harrington,[1,*] and Oleg Mitrofanov[2]

[1]Department of Material Science & Engineering, Rutgers University, 607 Taylor Road, Piscataway, New Jersey 08854, USA

[2]Bell Laboratories, Lucent Technologies, 600 Mountain Avenue, Murray Hill, New Jersey 07974, USA

**Corresponding author: jaharrin@rutgers.edu*

We have applied techniques developed for IR waveguides to fabricate Ag/polystyrene (PS) -coated hollow glass waveguides (HGWs) for transmission of terahertz radiation. A loss of 0.95 dB/m at 119 μm (2.5 THz) was obtained for a 2 mm bore, 90 cm long Ag/PS HGW. We found that TE modes are supported in HGWs with thin PS films, while hybrid (HE) modes dominate when PS film thickness increases. The lowest losses are obtained for the thicker PS films and the propagation of the HE modes. © 2007 Optical Society of America

2.4 PROPAGATION LOSSES

2.4.1 Metallic Hollow Core Waveguides

In 1964, Marcatili and Schmeltzer were the first to attempt to fully describe mathematically the transmission of IR radiation within hollow circular waveguides.

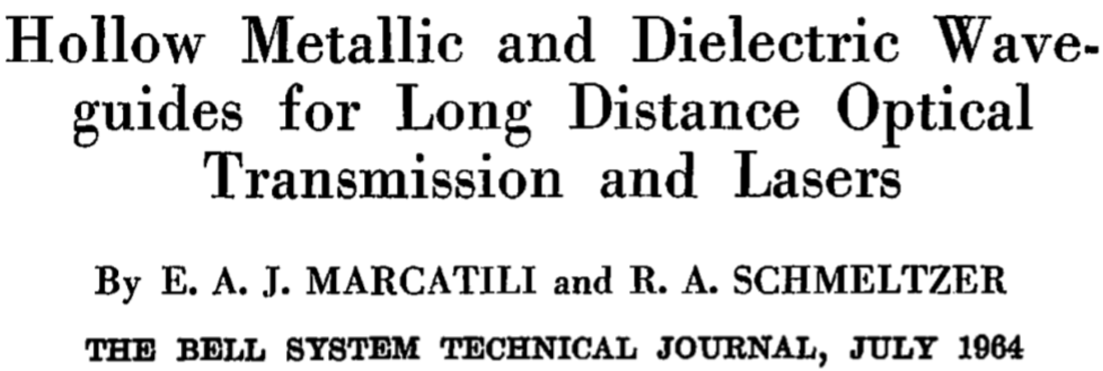
Hollow Metallic and Dielectric Waveguides for Long Distance Optical Transmission and Lasers

By E. A. J. MARCATILI and R. A. SCHMELTZER

THE BELL SYSTEM TECHNICAL JOURNAL, JULY 1964

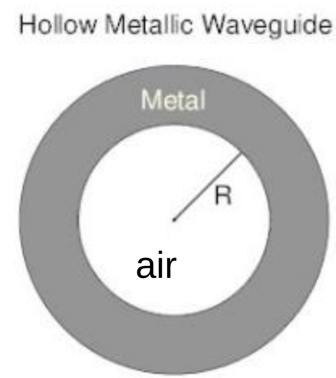

They developed a theoretical understanding of IR transmission in both metallic and dielectric cylindrical HWs.

Their effort on metallic WGs was motivated by the fact that the reflecting metal cannot be described as a conductor in the IR, as it can be at microwave frequencies.

They began describing the material using the complex refractive index which takes into account the large dielectric constant at optical frequencies.

2.4 PROPAGATION LOSSES

2.4.1 Metallic Hollow Core Waveguides

Marcatili and Schmeltzer began with two assumptions to simplify the calculations and more realistically describe the transmission behavior.

The first assumption is:

$$k_0 a = \frac{2\pi a}{\lambda} \gg m^{th} \text{ root of } J_{n-1}(\kappa a)$$

a = inner radius of waveguide

TE_{0m} modes → $\kappa a > m^{th}$ root of $J_0(\kappa a)$

HE_{1m} modes → $\kappa a > m^{th}$ root of $J_1(\kappa a)$

$$\kappa^2 = k_o^2 n^2 - \beta^2$$

β is the $\hat{z}$ - component of the wavevector k in the waveguide

This expression ensures the wavelength is much smaller than the internal radius of the tube and therefore essentially all the propagating energy is contained within the tube and strikes the walls at grazing angles so that there is minimal reflection loss.

The second assumption is:

$$\left|\left(\frac{\beta}{k_0}\right) - 1\right| \ll 1$$

This expression ensures only low loss modes, which have propagation constants approximately equal to that of the free space propagation constant k_0 are considered.

2.4 PROPAGATION LOSSES

2.4.1 Metallic Hollow Core Waveguides

It is accepted that all modes (transverse electric (TE), transverse magnetic (TM), hybrid modes) can be propagated within the hollow core waveguide.

Thus, the starting point is the general characteristic equation we found for step-index circular waveguide (**Chapter 1, Slide 36**):

$$\frac{\beta^2 \upsilon^2}{a^2}\left[\frac{1}{\gamma^2}+\frac{1}{\kappa^2}\right]^2 = \left[\frac{J'_\nu(\kappa a)}{\kappa J_\nu(\kappa a)}+\frac{K'_\nu(\gamma a)}{\gamma K_\nu(\gamma a)}\right]\cdot\left[\frac{k_o^2 n_{core}^2 J'_\nu(\kappa a)}{\kappa J_\nu(\kappa a)}+\frac{k_o^2 n_{clad}^2 K'_\nu(\gamma a)}{\gamma K_\nu(\gamma a)}\right]$$

For an HCW, $n_{core} = 1$:

$$\frac{\beta^2 \upsilon^2}{a^2}\left[\frac{1}{\gamma^2}+\frac{1}{\kappa^2}\right]^2 = \left[\frac{J'_\nu(\kappa a)}{\kappa J_\nu(\kappa a)}+\frac{K'_\nu(\gamma a)}{\gamma K_\nu(\gamma a)}\right]\cdot\left[\frac{k_o^2 J'_\nu(\kappa a)}{\kappa J_\nu(\kappa a)}+\frac{k_o^2 n_{clad}^2 K'_\nu(\gamma a)}{\gamma K_\nu(\gamma a)}\right]$$

For the case where υ = 0, that means we are considering only **TE_{0m}** and **TM_{0m}** modes:

$$\left[\frac{J'_\nu(\kappa a)}{\kappa J_\nu(\kappa a)}+\frac{K'_\nu(\gamma a)}{\gamma K_\nu(\gamma a)}\right]\cdot\left[\frac{k_o^2 J'_\nu(\kappa a)}{\kappa J_\nu(\kappa a)}+\frac{k_o^2 n_{clad}^2 K'_\nu(\gamma a)}{\gamma K_\nu(\gamma a)}\right] = 0$$

2.4 PROPAGATION LOSSES

2.4.1 Metallic Hollow Core Waveguides

$$\left[\frac{J'_\nu(\kappa a)}{\kappa J_\nu(\kappa a)} + \frac{K'_\nu(\gamma a)}{\gamma K_\nu(\gamma a)}\right] \cdot \left[\frac{k_o^2 J'_\nu(\kappa a)}{\kappa J_\nu(\kappa a)} + \frac{k_o^2 n_{clad}^2 K'_\nu(\gamma a)}{\gamma K_\nu(\gamma a)}\right] = 0$$

Assuming that the propagating energy is contained almost all within the tube, thus it makes sense to assess that κ must be real.

As a conseguence, γ is immaginary .

$$\kappa^2 = k_o^2 n_{clad}^2 - \beta^2$$
$$\gamma^2 = \beta^2 - k_o^2 n_{clad}^2$$

For large arguments γr, $K_\nu(i\gamma r)$ can be approximated as (**Chapter 1**, **Slide 22**).

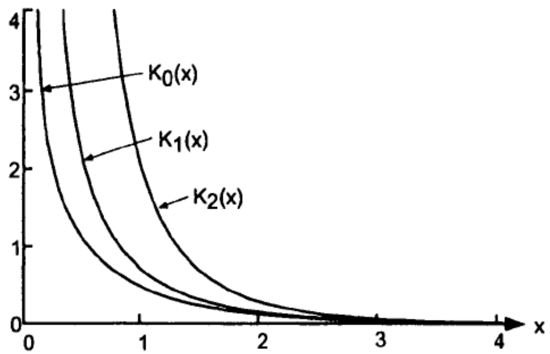

$$K_\nu(\gamma r) \approx \frac{e^{-i\gamma r}}{\sqrt{2\pi\, i\gamma r}}$$

Thus, the ratio can be approximated:

$$\frac{K'_\nu(\gamma a)}{K_\nu(\gamma a)} \approx i$$

Note: the derivative is of variable γr, an then calculated at the point $\gamma r = \gamma a$

2.4 PROPAGATION LOSSES

2.4.1 Metallic Hollow Core Waveguides

$$\left[\frac{J'_{\nu}(\kappa a)}{\kappa J_{\nu}(\kappa a)} + \frac{K'_{\nu}(\gamma a)}{\gamma K_{\nu}(\gamma a)}\right] \cdot \left[\frac{k_o^2 J'_{\nu}(\kappa a)}{\kappa J_{\nu}(\kappa a)} + \frac{k_0^2 n_{clad}^2 K'_{\nu}(\gamma a)}{\gamma K_{\nu}(\gamma a)}\right] = 0$$

$$\frac{K'_{\nu}(\gamma a)}{K_{\nu}(\gamma a)} \approx i$$

The characteristic equation becomes:

$$\left[\frac{J'_{\nu}(\kappa a)}{\kappa J_{\nu}(\kappa a)} + \frac{i}{\gamma}\right] \cdot \left[\frac{k_o^2 J'_{\nu}(\kappa a)}{\kappa J_{\nu}(\kappa a)} + \frac{k_o^2 n_{clad}^2 i}{\gamma}\right] = 0$$

Let us focus our attention on γ :

$$-\gamma^2 = k_0^2 {n_{clad}}^2 - \beta^2 = k_o^2\left({n_{clad}}^2 - \frac{\beta^2}{k_o^2}\right)$$

Adding and subtracting 1 in the round bracket (**Note:** γ is imaginary):

$$-\gamma = k_0\sqrt{{n_{clad}}^2 - \left(\frac{\beta^2}{k_o^2} - 1\right) - 1}$$

2.4 PROPAGATION LOSSES

2.4.1 Metallic Hollow Core Waveguides

$$-\gamma = k_0 \sqrt{{n_{clad}}^2 - \left(\frac{\beta^2}{k_o^2} - 1\right) - 1}$$

With the assumption that $\left|\left(\frac{\beta}{k_0}\right) - 1\right| \ll 1$, the term in the round bracket can be neglected, leading to:

$$-\gamma = k_0 \sqrt{{n_{clad}}^2 - 1}$$

From the characteristic equation:

$$\left[\frac{J'_\nu(\kappa a)}{\kappa J_\nu(\kappa a)} + \frac{i}{\gamma}\right] \cdot \left[\frac{k_o^2 J'_\nu(\kappa a)}{\kappa J_\nu(\kappa a)} + \frac{k_o^2 n_{clad}^2 i}{\gamma}\right] = 0$$

The condition for **TE_{0m}** modes are determined by imposing to zero the first square bracket (**Chapter 1**, **Slide 37**):

$$\left[\frac{J'_\nu(\kappa a)}{\kappa J_\nu(\kappa a)} + \frac{i}{\gamma}\right] = 0$$

2.4 PROPAGATION LOSSES

2.4.1 Metallic Hollow Core Waveguides

$$\left[\frac{J'_\nu(\kappa a)}{\kappa J_\nu(\kappa a)} + \frac{i}{\gamma}\right] = 0$$

By using the following Bessel function identity for $\nu = 0$ (**Chapter 1**, **Slide 46**):

$$\frac{J'_\nu(\kappa a)}{J_\nu(\kappa a)} = \frac{J_{\nu-1}(\kappa a)}{J_\nu(\kappa a)}$$

The characteristics equation for **TE_{0m}** modes is:

$$-\gamma = k_0\sqrt{{n_{clad}}^2 - 1}$$

$$J_{\nu-1}(\kappa a) = -i\frac{\kappa}{\gamma}J_\nu(\kappa a) = i\left(\frac{\kappa}{k_o}\right)J_\nu(\kappa a)\frac{1}{\sqrt{{n_{clad}}^2 - 1}}$$

The condition for **TM_{0m}** modes are determined by imposing to zero the second square bracket (**Chapter 1**, **Slide 37**):

$$\left[\frac{J'_\nu(\kappa a)}{\kappa J_\nu(\kappa a)} + \frac{i}{\gamma}\right] \cdot \left[\frac{k_o^2 J'_\nu(\kappa a)}{\kappa J_\nu(\kappa a)} + \frac{k_o^2 n_{clad}^2 i}{\gamma}\right] = 0$$

$$\left[\frac{k_o^2 J_{\nu-1}(\kappa a)}{\kappa J_\nu(\kappa a)} + \frac{k_o^2 n_{clad}^2 i}{\gamma}\right] = 0$$

2.4 PROPAGATION LOSSES

2.4.1 Metallic Hollow Core Waveguides

$$\left[\frac{k_o^2 J_{\nu-1}(\kappa a)}{\kappa J_\nu(\kappa a)} + \frac{k_o^2 n_{clad}^2 i}{\gamma}\right] = 0$$

As for **TE$_{0m}$** modes, by using:

$$\frac{J'_\nu(\kappa a)}{J_\nu(\kappa a)} = \frac{J_{\nu-1}(\kappa a)}{J_\nu(\kappa a)} \qquad -\gamma = k_0\sqrt{n_{clad}{}^2 - 1}$$

the characteristics equation for **TM$_{0m}$** modes is:

$$J_{\nu-1}(\kappa a) = i\left(\frac{\kappa}{k_o}\right) J_\nu(\kappa a) \frac{n_{clad}^2}{\sqrt{n_{clad}{}^2 - 1}}$$

for **TE$_{0m}$** modes

$$J_{\nu-1}(\kappa a) = i\left(\frac{\kappa}{k_o}\right) J_\nu(\kappa a) \frac{1}{\sqrt{n_{clad}{}^2 - 1}}$$

Combining the expressions found for **TE$_{0m}$** e **TM$_{0m}$** modes, we can introduce $\nu_{n_{clad}}$:

$$J_{\nu-1}(\kappa a) = i\left(\frac{\kappa}{k_o}\right) J_\nu(\kappa a)\nu_{n_{clad}} \quad \text{where} \quad \nu_{n_{clad}} = \begin{cases} \dfrac{1}{\sqrt{n_{clad}{}^2 - 1}} & \text{for } \mathbf{TE_{0m}} \\ \dfrac{n_{clad}^2}{\sqrt{n_{clad}{}^2 - 1}} & \text{for } \mathbf{TM_{0m}} \end{cases}$$

2.4 PROPAGATION LOSSES

2.4.1 Metallic Hollow Core Waveguides

$$\frac{\beta^2 \upsilon^2}{a^2}\left[\frac{1}{\gamma^2}+\frac{1}{\kappa^2}\right]^2 = \left[\frac{J'_\nu(\kappa a)}{\kappa J_\nu(\kappa a)}+\frac{K'_\nu(\gamma a)}{\gamma K_\nu(\gamma a)}\right]\cdot\left[\frac{k_o^2 J'_\nu(\kappa a)}{\kappa J_\nu(\kappa a)}+\frac{k_o^2 n_{clad}^2 K'_\nu(\gamma a)}{\gamma K_\nu(\gamma a)}\right]$$

For hybrid modes **HE$_{vm}$** we need to re-start from the characteristic equation with $\upsilon \neq 0$ and with the approximation $\frac{K'_\nu(\gamma a)}{K_\nu(\gamma a)} \approx i$:

$$\left[\frac{J'_\nu(\kappa a)}{\kappa J_\nu(\kappa a)}+\frac{i}{\gamma}\right]\cdot\left[\frac{k_o^2 J'_\nu(\kappa a)}{\kappa J_\nu(\kappa a)}+\frac{k_o^2 n_{clad}^2 i}{\gamma}\right] = \frac{\beta^2 \upsilon^2}{a^2}\left[\frac{1}{\gamma^2}+\frac{1}{\kappa^2}\right]^2$$

By using the Bessel function identity for $\upsilon \neq 0$ (**Chapter 1**, **Slide 46**):

$$\frac{J'_\nu(\kappa a)}{J_\nu(\kappa a)} = \frac{J_{\nu-1}(\kappa a)}{J_\nu(\kappa a)} - \frac{\nu}{a\kappa}$$

the characteristic equation becomes:

$$\left[\frac{J_{\nu-1}(\kappa a)}{\kappa J_\nu(\kappa a)} - \frac{\nu}{a\kappa^2}+\frac{i}{\gamma}\right]\cdot\left[\frac{k_o^2 J_{\nu-1}(\kappa a)}{\kappa J_\nu(\kappa a)} - \frac{k_o^2 \nu}{a\kappa^2}+\frac{k_o^2 n_{clad}^2 i}{\gamma}\right] = \frac{\beta^2 \upsilon^2}{a^2}\left[\frac{1}{\gamma^2}+\frac{1}{\kappa^2}\right]^2$$

2.4 PROPAGATION LOSSES

2.4.1 Metallic Hollow Core Waveguides

$$\left[\frac{J_{\nu-1}(\kappa a)}{\kappa J_\nu(\kappa a)} - \frac{\nu}{a\kappa^2} + \frac{i}{\gamma}\right] \cdot \left[\frac{\boldsymbol{k_0^2} J_{\nu-1}(\kappa a)}{\kappa J_\nu(\kappa a)} - \frac{\boldsymbol{k_0^2}\nu}{a\kappa^2} + \frac{\boldsymbol{k_0^2} n_{clad}^2 i}{\gamma}\right] = \frac{\beta^2 \upsilon^2}{a^2}\left[\frac{1}{\gamma^2} + \frac{1}{\kappa^2}\right]^2$$

Let's move $\boldsymbol{k_o^2}$ on the right-hand side:

$$\left[\frac{J_{\nu-1}(\kappa a)}{\kappa J_\nu(\kappa a)} - \frac{\nu}{a\kappa^2} + \frac{i}{\gamma}\right] \cdot \left[\frac{J_{\nu-1}(\kappa a)}{\kappa J_\nu(\kappa a)} - \frac{\nu}{a\kappa^2} + \frac{n_{clad}^2 i}{\gamma}\right] = \frac{\beta^2 \upsilon^2}{\boldsymbol{k_0^2} a^2}\left[\frac{1}{\gamma^2} + \frac{1}{\kappa^2}\right]^2$$

Since $|\gamma a| \gg 1$, one derive that with a fixed:

$$\left|\frac{1}{\gamma}\right| \ll a$$

Thus, solving the binomial square on right-hand side, all powers of γ larger than one shall be neglected.

This leads to:

$$\left[\frac{J_{\nu-1}(\kappa a)}{\kappa J_\nu(\kappa a)} - \frac{\nu}{a\kappa^2} + \frac{i}{\gamma}\right] \cdot \left[\frac{J_{\nu-1}(\kappa a)}{\kappa J_\nu(\kappa a)} - \frac{\nu}{a\kappa^2} + \frac{n_{clad}^2 i}{\gamma}\right] = \frac{\beta^2 \upsilon^2}{k_o^2 a^2 \kappa^4}$$

2.4 PROPAGATION LOSSES

2.4.1 Metallic Hollow Core Waveguides

$$\left[\frac{J_{\nu-1}(\kappa a)}{\kappa J_\nu(\kappa a)} - \frac{\nu}{a\kappa^2} + \frac{i}{\gamma}\right] \cdot \left[\frac{J_{\nu-1}(\kappa a)}{\kappa J_\nu(\kappa a)} - \frac{\nu}{a\kappa^2} + \frac{n_{clad}^2 i}{\gamma}\right] = \frac{\boldsymbol{\beta^2} \upsilon^2}{\boldsymbol{k_o^2} a^2 \kappa^4}$$

Again, since $\left|\left(\frac{\beta}{k_0}\right) - 1\right| \ll 1$, the ratio $\frac{\boldsymbol{\beta^2}}{\boldsymbol{k_o^2}} \approx 1$.

$$\left[\frac{J_{\nu-1}(\kappa a)}{\kappa J_\nu(\kappa a)} - \frac{\nu}{a\kappa^2} + \frac{i}{\gamma}\right] \cdot \left[\frac{J_{\nu-1}(\kappa a)}{\kappa J_\nu(\kappa a)} - \frac{\nu}{a\kappa^2} + \frac{n_{clad}^2 i}{\gamma}\right] = \frac{\upsilon^2}{a^2 \kappa^4}$$

Let's expand the product on left-hand side:

$$\left(\frac{J_{\nu-1}(\kappa a)}{\kappa J_\nu(\kappa a)} - \frac{\nu}{a\kappa^2}\right)^2 + \left(\frac{J_{\nu-1}(\kappa a)}{\kappa J_\nu(\kappa a)} - \frac{\nu}{a\kappa^2}\right)\frac{i}{\gamma}\left(n_{clad}^2 + 1\right) - \frac{n_{clad}^2}{\gamma^2} = \frac{\upsilon^2}{a^2 \kappa^4}$$

Neglecting the last term on left-hand side because proportional to $\frac{1}{\gamma^2}$:

$$\left(\frac{J_{\nu-1}(\kappa a)}{\kappa J_\nu(\kappa a)} - \frac{\nu}{a\kappa^2}\right)^2 + \left(\frac{J_{\nu-1}(\kappa a)}{\kappa J_\nu(\kappa a)} - \frac{\nu}{a\kappa^2}\right)\frac{i}{\gamma}\left(n_{clad}^2 + 1\right) = \frac{\upsilon^2}{a^2 \kappa^4}$$

2.4 PROPAGATION LOSSES

2.4.1 Metallic Hollow Core Waveguides

$$\left(\frac{J_{\nu-1}(\kappa a)}{\kappa J_\nu(\kappa a)} - \frac{\nu}{a\kappa^2}\right)^2 + \left(\frac{J_{\nu-1}(\kappa a)}{\kappa J_\nu(\kappa a)} - \frac{\nu}{a\kappa^2}\right)\frac{i}{\gamma}\left(n_{clad}^2 + 1\right) = \frac{\upsilon^2}{a^2\kappa^4}$$

Expanding the first binomial square on left-hand side, the square of the second term will be the same as the term on the right-hand side:

$$\left(\frac{J_{\nu-1}(\kappa a)}{\kappa J_\nu(\kappa a)}\right)^2 - 2\frac{J_{\nu-1}(\kappa a)}{\kappa J_\nu(\kappa a)}\frac{\nu}{a\kappa^2} + \left(\frac{J_{\nu-1}(\kappa a)}{\kappa J_\nu(\kappa a)} - \frac{\nu}{a\kappa^2}\right)\frac{i}{\gamma}\left(n_{clad}^2 + 1\right) = 0$$

Let us focus our attention on the ratio $\frac{J_{\nu-1}(\kappa a)}{J_\nu(\kappa a)}$.

It is easy to show that, for larger values of κa and far from the zeros of $J_\nu(\kappa a)$, the ratio $\frac{J_{\nu-1}(\kappa a)}{J_\nu(\kappa a)} \approx 0$

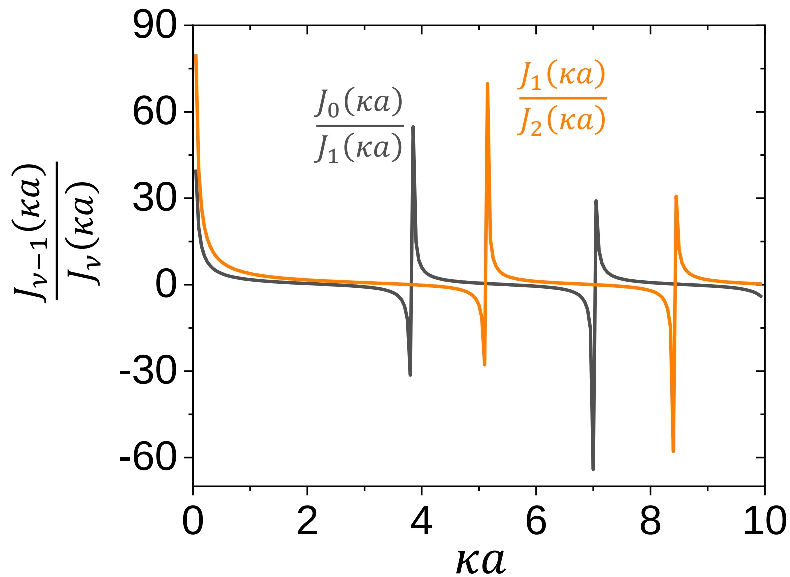

2.4 PROPAGATION LOSSES

2.4.1 Metallic Hollow Core Waveguides

$$\left(\frac{J_{\nu-1}(\kappa a)}{\kappa J_\nu(\kappa a)}\right)^2 - 2\frac{J_{\nu-1}(\kappa a)}{\kappa J_\nu(\kappa a)}\frac{\nu}{a\kappa^2} + \left(\frac{J_{\nu-1}(\kappa a)}{\kappa J_\nu(\kappa a)} - \frac{\nu}{a\kappa^2}\right)\frac{i}{\gamma}\left(n_{clad}^2 + 1\right) = 0$$

Thus, we can neglect the first term:

$$-2\frac{J_{\nu-1}(\kappa a)}{\kappa J_\nu(\kappa a)}\frac{\nu}{a\kappa^2} + \left(\frac{J_{\nu-1}(\kappa a)}{\kappa J_\nu(\kappa a)} - \frac{\nu}{a\kappa^2}\right)\frac{i}{\gamma}\left(n_{clad}^2 + 1\right) = 0$$

Solving the product of the second term:

$$-2\frac{J_{\nu-1}(\kappa a)}{\kappa J_\nu(\kappa a)}\frac{\nu}{a\kappa^2} + \frac{J_{\nu-1}(\kappa a)}{\kappa J_\nu(\kappa a)}\frac{i}{\gamma}\left(n_{clad}^2 + 1\right) - \frac{\nu}{a\kappa^2}\frac{i}{\gamma}\left(n_{clad}^2 + 1\right) = 0$$

The second term can be neglected because since both $\frac{J_{\nu-1}(\kappa a)}{J_\nu(\kappa a)}$ and $\frac{1}{\gamma}$ are small:

$$-2\frac{J_{\nu-1}(\kappa a)}{\kappa J_\nu(\kappa a)}\frac{\nu}{a\kappa^2} - \frac{\nu}{a\kappa^2}\frac{i}{\gamma}\left(n_{clad}^2 + 1\right) = 0$$

2.4 PROPAGATION LOSSES

2.4.1 Metallic Hollow Core Waveguides

$$-2\frac{J_{\nu-1}(\kappa a)}{\kappa J_\nu(\kappa a)}\frac{\nu}{a\kappa^2}-\frac{\nu}{a\kappa^2}\frac{i}{\gamma}\left(n_{clad}^2+1\right)=0$$

that can simplify as:

$$-2\frac{J_{\nu-1}(\kappa a)}{\kappa J_\nu(\kappa a)}-\frac{i}{\gamma}\left(n_{clad}^2+1\right)=0$$

By replacing the expression found for γ:

$$-\gamma=k_0\sqrt{n_{clad}{}^2-1}$$

$$-2\frac{J_{\nu-1}(\kappa a)}{\kappa J_\nu(\kappa a)}-\frac{i\left(n_{clad}^2+1\right)}{k_0\sqrt{n_{clad}{}^2-1}}=0$$

leading to:

$$J_{\nu-1}(\kappa a)=i\left(\frac{\kappa}{k_o}\right)J_\nu(\kappa a)\frac{(n_{clad}^2+1)}{2\sqrt{n_{clad}{}^2-1}}$$

2.4 PROPAGATION LOSSES

2.4.1 Metallic Hollow Core Waveguides

We can complete now the expression found for **TE$_{0m}$** e **TM$_{0m}$** modes :

$$J_{\nu-1}(\kappa a) = i\left(\frac{\kappa}{k_o}\right) J_\nu(\kappa a)\nu_{n_{clad}} \quad \text{where} \quad \nu_{n_{clad}} = \begin{cases} \dfrac{1}{\sqrt{{n_{clad}}^2-1}} & \text{for TE}_{0m} \\ \dfrac{n_{clad}^2}{\sqrt{{n_{clad}}^2-1}} & \text{for TM}_{0m} \end{cases}$$

$$J_{\nu-1}(\kappa a) = i\left(\frac{\kappa}{k_o}\right) J_\nu(\kappa a)\frac{(n_{clad}^2+1)}{2\sqrt{{n_{clad}}^2-1}} \quad \text{for HE}_{\nu m}$$

with:

$$J_{\nu-1}(\kappa a) = i\left(\frac{\kappa}{k_o}\right) J_\nu(\kappa a)\nu_{n_{clad}} \quad \textit{where} \quad \nu_{n_{clad}} = \begin{cases} \dfrac{1}{\sqrt{{n_{clad}}^2-1}} & \text{for TE}_{0m} \\ \dfrac{n_{clad}^2}{\sqrt{{n_{clad}}^2-1}} & \text{for TM}_{0m} \\ \dfrac{(n_{clad}^2+1)}{2\sqrt{{n_{clad}}^2-1}} & \text{for HE}_{\nu m} \end{cases}$$

2.4 PROPAGATION LOSSES

2.4.1 Metallic Hollow Core Waveguides

$$J_{\nu-1}(\kappa a) = i\left(\frac{\kappa}{k_o}\right)J_\nu(\kappa a)\nu_{n_{clad}}$$

To solve the characteristic equation for κa we notice that because of

$$k_0 a = \frac{2\pi a}{\lambda} \gg m^{th} \text{ root of } J_{\nu-1}(\kappa a)$$

$$\kappa^2 = k_o^2 - \beta^2$$

$$\left|\left(\frac{\beta}{k_0}\right) - 1\right| \ll 1$$

the right-hand side of characteristic equation

$$\frac{J_{\nu-1}(\kappa a)}{J_\nu(\kappa a)} = i\left(\frac{\kappa a}{k_o a}\right)\nu_{n_{clad}} \approx 0$$

is close to zero.

This means that when κa is close to m^{th} root of $J_{\nu-1}(\kappa a)$, the right-hand side $i\left(\frac{\kappa a}{k_o a}\right)\nu_{n_{clad}}$ will be proportional to the first term of the perturbation around $\kappa a = u_{\nu m}$, where $u_{\nu m}$ is the m^{th} root of $J_{\nu-1}(\kappa a)$:

$$\kappa a \approx u_{\nu m} - i\left(\frac{u_{\nu m}}{k_o a}\right)\nu_{n_{clad}} = u_{\nu m}\left(1 - \frac{i\nu_{n_{clad}}}{k_o a}\right)$$

2.4 PROPAGATION LOSSES

2.4.1 Metallic Hollow Core Waveguides

$$\kappa a \approx u_{vm} - i\left(\frac{u_{vm}}{k_o a}\right)\nu_{n_{clad}} = u_{vm}\left(1 - \frac{i\nu_{n_{clad}}}{k_o a}\right)$$

The propagation constant β can be determined by using $\kappa^2 = k_o^2 - \beta^2$

By squaring both sides of the expression for κa:

$$\kappa^2 = \frac{1}{a^2}{u_{vm}}^2\left(1 - \frac{i\nu_{n_{clad}}}{k_o a}\right)^2$$

Expanding the binomial square on right-hand side and neglecting the quadratic term $\left(\frac{\nu_{n_{clad}}}{k_o a}\right)^2$, we have:

$$\kappa^2 \approx \frac{1}{a^2}{u_{vm}}^2\left(1 - 2\frac{i\nu_{n_{clad}}}{k_o a}\right)$$

Including the latter in the expression for the propagation constant β:

$$\beta^2 = k_0^2 - \kappa^2 \approx k_0^2 - \frac{1}{a^2}{u_{vm}}^2\left(1 - 2\frac{i\nu_{n_{clad}}}{k_o a}\right)$$

2.4 PROPAGATION LOSSES

2.4.1 Metallic Hollow Core Waveguides

$$\beta^2 = k_0^2 - \kappa^2 \approx k_0^2 - \frac{1}{a^2} {u_{vm}}^2 \left(1 - 2\frac{i\nu_{n_{clad}}}{k_o a}\right)$$

By collecting k_0^2 as a common factor:

$$\beta^2 = k_0^2 \left[1 - \frac{{u_{vm}}^2}{a^2 k_0^2}\left(1 - 2\frac{i\nu_{n_{clad}}}{k_o a}\right)\right]$$

Thus we have:

$$\beta = k_0 \sqrt{1 - \frac{{u_{vm}}^2}{a^2 k_0^2}\left(1 - 2\frac{i\nu_{n_{clad}}}{k_o a}\right)} = k_0\sqrt{1 - x}$$

$$x = \frac{{u_{vm}}^2}{a^2 k_0^2}\left(1 - 2\frac{i\nu_{n_{clad}}}{k_o a}\right)$$

By considering a Taylor expansion of the function $\sqrt{1-x}$ around $x = 0$:

$$\sqrt{1-x} \approx 1 - \frac{1}{2}x$$

Finally we have:

$$\beta \approx k_0 \left[1 - \frac{1}{2}\frac{{u_{vm}}^2}{a^2 k_0^2}\left(1 - 2\frac{i\nu_{n_{clad}}}{k_o a}\right)\right]$$

2.4 PROPAGATION LOSSES

2.4.1 Metallic Hollow Core Waveguides

$$\beta \approx k_0 \left[1 - \frac{1}{2} \frac{{u_{\nu m}}^2}{a^2 k_0^2} \left(1 - 2 \frac{i \nu_{n_{clad}}}{k_o a} \right) \right]$$

The **longitudinal field** $E_z(r, \phi, z)$ in the region $r < a$ has the form (**Chapter 1**, **Slide 24**):

$$E_z(r, \phi, z) = A J_\nu(\kappa r) e^{i\nu\phi} e^{-i\beta z} + c.c.$$

and radial and azimuthal fields can be written as a function the longitudinal components (**Chapter 1**, **Slide 27**):

Being the intensity $I \propto {E_z}^* E_z$, the imaginary part of β is related the attenuation of the electric field while it is propagating, thus it is a measure of propagation losses $\alpha_{\nu m}$.

$$\alpha_{\nu m} = Im(\beta) = \left(\frac{u_{\nu m}}{2\pi} \right)^2 \frac{\lambda^2}{a^3} \mathcal{R}e \begin{cases} \dfrac{1}{\sqrt{{n_{clad}}^2 - 1}} & \text{for } \mathbf{TE_{0m}} \\ \dfrac{n_{clad}^2}{\sqrt{{n_{clad}}^2 - 1}} & \text{for } \mathbf{TM_{0m}} \\ \dfrac{\left(n_{clad}^2 + 1 \right)}{2\sqrt{{n_{clad}}^2 - 1}} & \text{for } \mathbf{HE_{\nu m}} \end{cases}$$

$$k_0 = \frac{2\pi}{\lambda}$$

2.4 PROPAGATION LOSSES

2.4.1 Metallic Hollow Core Waveguides

$$\alpha_{vm} = Im(\beta) = \left(\frac{u_{vm}}{2\pi}\right)^2 \frac{\lambda^2}{a^3} \mathcal{R}e \begin{cases} \dfrac{1}{\sqrt{{n_{clad}}^2 - 1}} & \text{for } \mathrm{TE_{0m}} \\ \dfrac{n_{clad}^2}{\sqrt{{n_{clad}}^2 - 1}} & \text{for } \mathrm{TM_{0m}} \\ \dfrac{\left(n_{clad}^2 + 1\right)}{2\sqrt{{n_{clad}}^2 - 1}} & \text{for } \mathrm{HE}_{\nu m} \end{cases}$$

This result by Marcantili and Schmeltzer is used almost exclusively to calculate the loss for straight hollow waveguides made from an inner wall material with refractive index n_{clad}.

It is observed that α_{vm} depends on $\frac{\lambda^2}{a^3}$ and the loss increases as the square of the mode parameter u_{vm}, the m^{th} root of $J_{\nu-1}(\kappa a)$.

Since the intensity $I \propto {E_z}^* E_z$, the absorption coefficient will be $\alpha = 2\alpha_{vm}$.

Values for u_{vm} for some of the lowest-order modes

	$m = 1$	2	3	4
$v = 1$	2.405	5.52	8.654	11.796
2	3.832	7.016	10.173	13.324
3	5.136	8.417	11.62	14.796
4	6.380	9.761	13.015	16.223

2.4 PROPAGATION LOSSES

2.4.2 Metallic/Dielectric Hollow Core Waveguides

The losses in Marcantili and Schmeltzer waveguides that incorporate only one wall material with complex refractive index n_{clad} can be quite large.

To reduce the loss, it is necessary to somehow deposit thin films over the metallic layer to basically enhance the reflectivity over the metal, as discussed in **Section 2.3**.

Miyagi and Kawakami first proposed such multilayer structures in the early 1980s.

116 JOURNAL OF LIGHTWAVE TECHNOLOGY, VOL. LT-2, NO. 2, APRIL 1984

Design Theory of Dielectric-Coated Circular Metallic Waveguides for Infrared Transmission

MITSUNOBU MIYAGI AND SHOJIRO KAWAKAMI, MEMBER, IEEE

The theory of Miyagi and Kawakami gives result similar to that of Marcantili and Schmeltzer, but with an additional terms reflecting the properties of the dielectric layers used in the stack.

Marcantili and Schmeltzer

$$\alpha_{vm} = Im(\beta) = \left(\frac{u_{vm}}{2\pi}\right)^2 \frac{\lambda^2}{a^3}\, \mathcal{R}e \begin{cases} \dfrac{1}{\sqrt{{n_{clad}}^2 - 1}} & \text{for } \mathbf{TE_{0m}} \\ \dfrac{n_{clad}^2}{\sqrt{{n_{clad}}^2 - 1}} & \text{for } \mathbf{TM_{0m}} \\ \dfrac{(n_{clad}^2 + 1)}{2\sqrt{{n_{clad}}^2 - 1}} & \text{for } \mathbf{HE_{\nu m}} \end{cases}$$

2.4 PROPAGATION LOSSES

2.4.2 Metallic/Dielectric Hollow Core Waveguides

The explicit nature of α_{vm} is complicated, expecially when two materials and multilayers are used.

To illustrate the effect of dielectric films deposited on metallic layer, consider the easiest case of one dielectric film deposited on metallic layer.

Miyagi and Kawakami derived the following expression for the losses for the three modes as:

$$\alpha_{vm} = Im(\beta) = \left(\frac{u_{vm}}{2\pi}\right)^2 \frac{\lambda^2}{a^3}\left(\frac{n}{n^2+k^2}\right) \begin{cases} \left(1+\dfrac{n_d^2}{\sqrt{{n_d}^2-1}}\right) & \text{for } \mathbf{TE_{0m}} \\ \dfrac{n_d^2}{\sqrt{{n_d}^2-1}}\left(1+\dfrac{n_d^2}{\sqrt{{n_d}^2-1}}\right) & \text{for } \mathbf{TM_{0m}} \\ \dfrac{1}{2}\left(1+\dfrac{n_d^2}{\sqrt{{n_d}^2-1}}\right) & \text{for } \mathbf{HE_{\nu m}} \end{cases}$$

where n_d is the refractive index of dielectric and n and k are the real and the imaginary part of the refractive index of metallic layer.

2.4 PROPAGATION LOSSES

2.4.2 Metallic/Dielectric Hollow Core Waveguides

The lowest-loss modes can be now estimated for the lowest-order modes.

We just need to plot the argument in curly bracket as a function of n_d.

$$\alpha_{\nu m} = Im(\beta) = \left(\frac{u_{\nu m}}{2\pi}\right)^2 \frac{\lambda^2}{a^3} \left(\frac{n}{n^2+k^2}\right) \begin{cases} \left(1+\frac{n_d^2}{\sqrt{{n_d}^2-1}}\right) & \text{for } TE_{0m} \\ \frac{n_d^2}{\sqrt{{n_d}^2-1}}\left(1+\frac{n_d^2}{\sqrt{{n_d}^2-1}}\right) & \text{for } TM_{0m} \\ \frac{1}{2}\left(1+\frac{n_d^2}{\sqrt{{n_d}^2-1}}\right) & \text{for } HE_{\nu m} \end{cases}$$

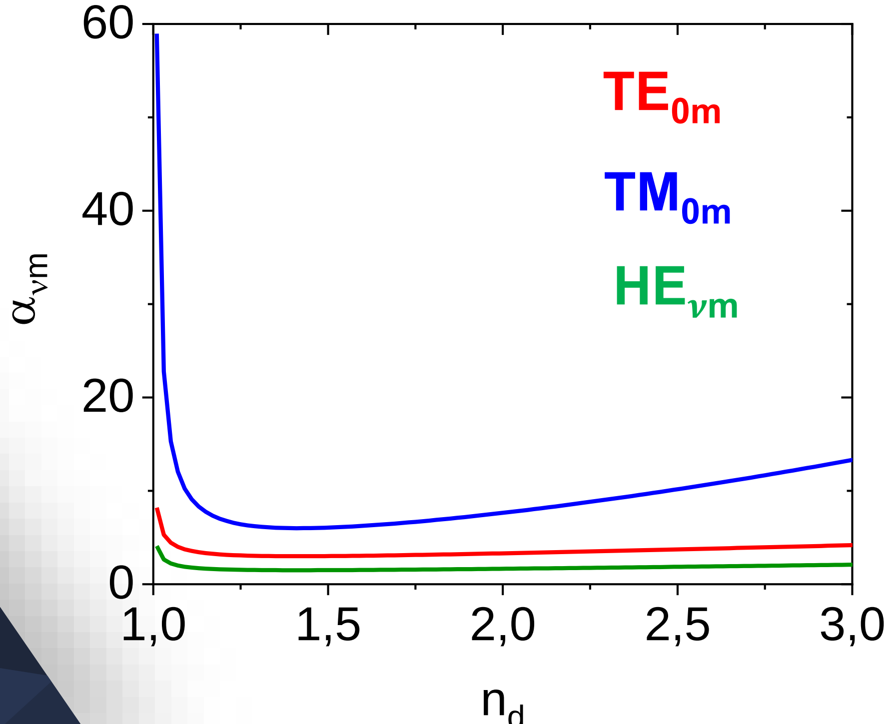

The fundamental HE_{11} is the lowest-loss mode

2.5 THE FUNDAMENTAL HYBRID MODE HE_{11}

The cut-off condition for the **HE_{11}** mode occurs at the first root of the Bessel function $J_1(\kappa a)$ (**Chapter 1, Slide 61**).

HE_{1m} modes → $\kappa a > m^{th}$ root of $J_1(\kappa a)$

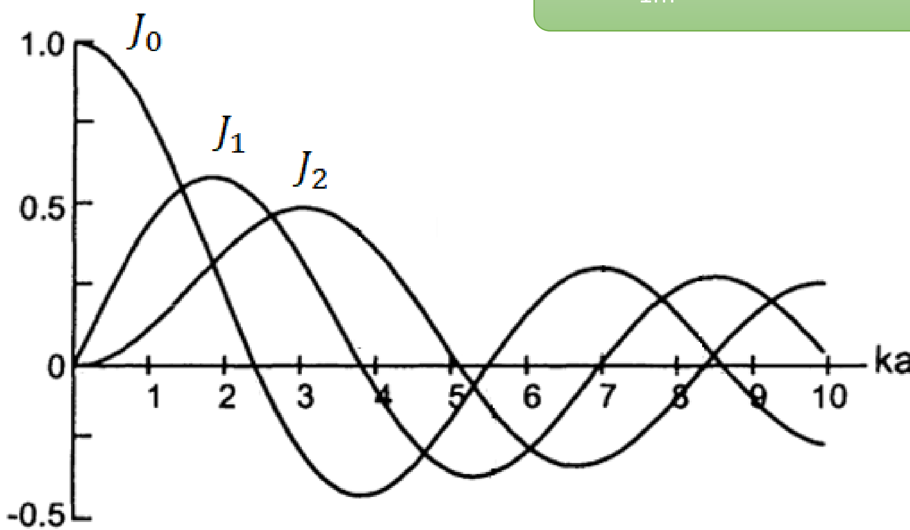

The first zero crossing of $J_1(\kappa a)$ occurs when $\kappa a = 0$ and gives the cutoff for **HE_{11}** mode.

Thus, the **HE_{11}** mode has no cut-off, and ceases to exist only when the core diameter is zero.

Which is the field distribution in the **HE_{11}** mode in the air core of HCW?

HE_{11} mode is a linearly polarized LP_{01} mode (**Chapter 1, Slide 61**).

2.5 THE FUNDAMENTAL HYBRID MODE HE_{11}

Since $\nu = 0$, then the electric field will be linearly polarized, with no node points.

Consider the general expression of longitudinal component of the electric field $E_z(r,\phi,z)$.

$$E_z(r,\phi,z) = \begin{cases} AJ_\nu(\kappa r)e^{i\nu\phi}e^{-i\beta z} + c.c. & r < a \\ CK_\nu(\gamma r)e^{i\nu\phi}e^{-i\beta z} + c.c. & r > a \end{cases}$$

Thus, the radial distribution of the **HE_{11}** mode ($\nu = 0$) for a metallic/dielectric waveguide can be approximated as:

$$E_z(r,z) = E_0 J_0\left(u_{1m}\frac{r}{a}\right)e^{-i\beta z} \quad \text{for } 0 < r < a$$

with $$Im(\beta) = \left(\frac{u_{\nu m}}{2\pi}\right)^2 \frac{\lambda^2}{a^3}\left(\frac{n}{n^2+k^2}\right)\frac{1}{2}\left(1 + \frac{n_d^2}{\sqrt{{n_d}^2-1}}\right)$$

The radial distribution of the **HE_{11}** mode is Gaussian-like.

2.6 LAUNCH CONDITIONS AND MODE COUPLING

The easiest way to couple radiation within an hollow core waveguide is to focus the laser beam at the waveguide entrance

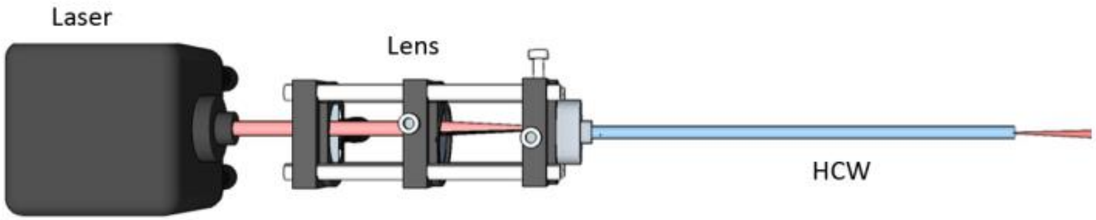

Considering a diffraction-limited collimated Gaussian laser beam with a radius w illuminating a lens with a focal length f and radius of curvature R, the waist radius w_0 at the focal plane is given by:

$$w_0 = \frac{w}{\sqrt{1 + \left(\frac{\pi w^2}{\lambda R}\right)^2}}$$

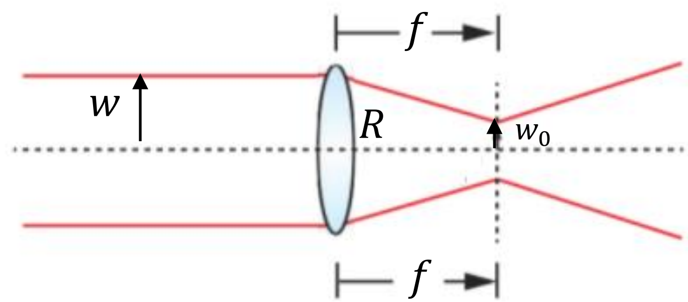

and the focal length f at different laser wavelengths λ is given by:

$$f = \frac{R}{1 + \left(\frac{\pi w^2}{\lambda R}\right)^2}$$

2.6 LAUNCH CONDITIONS AND MODE COUPLING

$$w_0 = \frac{w}{\sqrt{1 + \left(\frac{\pi w^2}{\lambda R}\right)^2}}$$

$$f = \frac{R}{1 + \left(\frac{\pi w^2}{\lambda R}\right)^2}$$

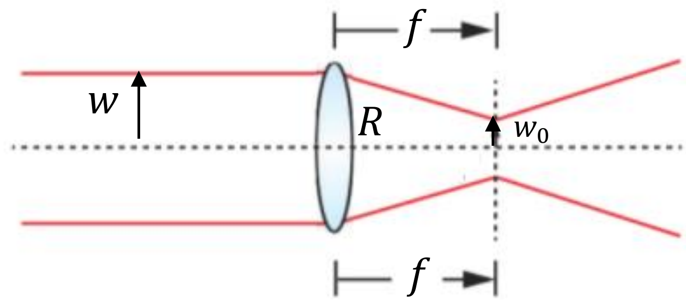

Hence, by measuring the size of the collimated beam, it is possible to estimate the waist radius at the waveguide entrance.

Thus, when optical coupling between a collimated laser beam and the HCW is obtained using a focusing lens, the propagation losses and the beam quality at the waveguide exit are affected by the input laser beam quality, the size as well as the focal length of the coupling lens.

When a Gaussian beam is focused into a hollow waveguide, which are **the best coupling conditions**?

The two highly desirable conditions for an excellent coupling conditions are:

- Low propagation loss
- Single mode beam output

2.6 LAUNCH CONDITIONS AND MODE COUPLING

Following these two requirements, the best coupling conditions can be obtained by maximizing the input laser mode coupling into the **HE_{11}** waveguide hybrid mode, providing the lowest theoretical losses and characterized by a Gaussian-like optical power distribution.

HE_{11}

Thus, it is desirable to know the launching conditions necessary to couple most of the input beam to this mode.

Assuming a Gaussian beam focused with a waist radius w_0 in the form of:

$$E(r) = E_0 e^{-\frac{r^2}{w_0^2}}$$

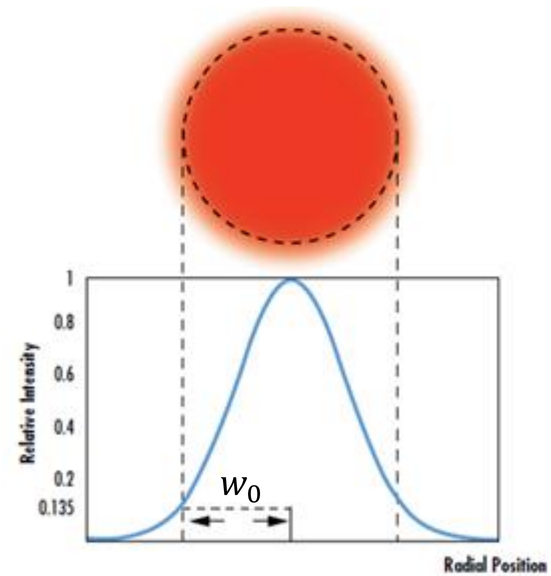

and the spatial profiles of the **HE_{11}** mode in a waveguide of bore radius a approximated by the zero order Bessel function:

$$J_0(r) = E_0 J_0\left(u_{1m}\frac{r}{a}\right)$$

2.6 LAUNCH CONDITIONS AND MODE COUPLING

$$E(r) = E_0 e^{-\frac{r^2}{w_0^2}}$$

$$J_0(r) = E_0 J_0\left(u_{1m}\frac{r}{a}\right)$$

The power coupling efficiency of the incident beam to the **HE_{11}** waveguide mode can be expressed by the overlap integral:

$$\eta_1 = \frac{\left[\int_0^a E(r) J_0(r) r dr\right]^2}{\int_0^\infty E^2(r)\, r dr \int_0^a {J_0}^2(r)\, r dr}$$

This equation describes the amount of power coupled to the **HE_{11}** waveguide mode for a given spot size to bore size ratio w_0/a.

With $\eta_1 \approx 1$, almost all input radiation is coupled in the waveguide, and it will propagate with low-loss.

The amount of power coupled with other modes will experience high losses; with a fiber sufficiently long, higher order modes will extinguish before reaching the waveguide output.

In other words, only the **HE_{11}** mode will survive, and the fiber will act as a modal filter for higher order modes, ensuring a single-mode output.

EXERCISES

Exercise 2

Consider a Gaussian laser beam focused into a hollow waveguide on axis. The waveguide bore radius is a and the waist radius at the waveguide entrance is w_0.

Calculate the beam waist to bore radius ratio, w_0/a, that maximizes the coupling efficiency η_1 with the lowest loss HE_{11} mode.

Suggestion:

- Use the definition of the coupling efficiency

$$\eta_1 = \frac{\left[\int_0^a E(r) J_0(r) r dr\right]^2}{\int_0^\infty E^2(r)\, rdr \int_0^a {J_0}^2(r)\, rdr}$$

together with the expressions for Gaussian and Bessel spatial profile:

$$E(r) = E_0 e^{-\frac{r^2}{w_0^2}} \qquad J_0(r) = E_0 J_0\left(u_{1m}\frac{r}{a}\right)$$